

Influence of Substituting Ni with Fe on Cycle Stabilities of as-Cast and as-Quenched $\text{La}_{0.7}\text{Mg}_{0.3}\text{Co}_{0.45}\text{Ni}_{2.55-x}\text{Fe}_x$ ($x = 0-0.4$) Electrode Alloys

Zhang Yanghuan^{1,2}, Li Baowei², Ren Huiping², Wu Zhongwang², Dong Xiaoping^{1,3}, Wang Xinlin¹

¹ Central Iron and Steel Research Institute, Beijing 100081, China; ² Inner Mongolia University of Science and Technology, Baotou 014010, China; ³ University of Science and Technology Beijing, Beijing 100083, China

Abstract: The electrode alloys $\text{La}_{0.7}\text{Mg}_{0.3}\text{Co}_{0.45}\text{Ni}_{2.55-x}\text{Fe}_x$ ($x = 0, 0.1, 0.2, 0.3, 0.4$) were prepared by casting and rapid quenching. The influences of the substitution of Fe for Ni on their cycle stabilities as well as their structures were investigated in detail. The results indicate that the substitution of Fe for Ni significantly improves the cycle stability of the alloys, and the positive impact of such a substitution on the cycle stability of the as-quenched alloy is much larger than that of the as-cast. All of the alloys have multiphase structures composed of two major phases, $(\text{La}, \text{Mg})\text{Ni}_3$ and LaNi_5 , and a residual phase LaNi_2 . The substitution of Fe for Ni helps the formation of a like amorphous structure in the as-quenched alloy. With the increase of Fe content, the grains in the as-quenched alloy are significantly refined, and the lattice constants and the cell volumes of the alloys are obviously enlarged.

Key words: La-Mg-Ni system electrode alloy; substituting Ni with Fe; rapid quenching; cycle stability; structure

Since the commercialization of small-sized Ni-MH cells in 1990, their turnout has rapidly grown and gained a good share of the rechargeable battery markets. In recent years, Ni-MH batteries used for motor vehicles (power battery in short below) have caught worldwide attention due to the tightening control of Cd pollution from Ni-Cd power battery in European community and other developed countries. However, none of the available electrode alloys including AB_3 and AB_2 types in use can meet the specification of the power battery owing to the limitation of their properties, such as the low discharge capacity of the AB_3 -type electrode alloy and the poor activation capability of the AB_2 -type Laves phase electrode alloy. Therefore, the research in this area has focused on finding new type electrode alloys with higher capacity and longer cycle life. Recently, R-Mg-Ni-based (here R is a rare earth element or Y, Ca) PuNi_3 -type alloys have been considered to be the most promising candidates owing to their high discharge capacities (360–410 $\text{mAh}\cdot\text{g}^{-1}$) and low production cost in spite of their

poor cycle stabilities. A lot of investigations on this kind of alloys have been performed by researchers in the world, and some very important results have been obtained. Kadir et al^[1-4], revealed that the alloy has a PuNi_3 -type rhombohedral structure. Kohno et al^[5], found that the $\text{La}_5\text{Mg}_2\text{Ni}_{23}$ -type electrode alloy $\text{La}_{0.7}\text{Mg}_{0.3}\text{Ni}_{2.8}\text{Co}_{0.5}$ has a capacity of 410 $\text{mAh}\cdot\text{g}^{-1}$, and good cycle stability during 30 charge-discharge cycles. Pan et al^[6], investigated the structures and electrochemical characteristics of the $\text{La}_{0.7}\text{Mg}_{0.3}(\text{Ni}_{0.85}\text{Co}_{0.15})_x$ ($x = 3.15-3.80$) alloy system and obtained a maximum discharge capacity of 398.4 $\text{mAh}\cdot\text{g}^{-1}$, but the cycle stability of the alloy needs to be improved further. Liao and Pan et al^[7,8], investigated the influences of element addition and substitution on the structure and electrochemical behaviour of the alloy, indicating that the addition and substitution of elements Al, Cu, Fe, Mn, Co and Zr significantly improves the electrochemical performances of the alloy. Although the investigations on the structure and electrochemical properties of the alloy have received very

Received date: June 25, 2008

Foundation items: Supported by 863 Program (2006AA05Z132); Science and Technology Planned Project of Inner Mongolia, China (20050205) and Natural Science Foundation of Inner Mongolia, China (200711020703)

Biography: Zhang Yanghuan, Professor, Department of Functional Material Research, Central Iron and Steel Research Institute, Beijing 100081, P. R. China, Tel: 0086-10-62187570; E-mail: zyh59@yahoo.com.cn

Copyright © 2009, Northwest Institute for Nonferrous Metal Research. Published by Elsevier BV. All rights reserved.

important progress, there is still a long way to go for the Mg₂Ni-type alloy to move from laboratory to market. The key challenge remains unchanged, i.e. how to improve its cycle stability. It is well known that the element substitution is one of the effective methods for improving the overall properties of the hydrogen storage alloys. In addition, the preparation technology is also vital for improving the performances of the alloys. Therefore, it is expected that the combination of an optimized amount of Fe substitution for Ni with a proper rapid quenching technique may lead to an alloy with high discharge capacity and good cycling stability. For this purpose, the effects of the substitution of Fe for Ni and rapid quenching on the cycle stabilities, structures and morphologies of the La_{0.7}Mg_{0.3}Co_{0.45}Ni_{2.55-x}Fe_x ($x=0-0.4$) electrode alloys were systematically investigated in this paper.

1 Experimental

The nominal compositions of the experimental alloys were La_{0.7}Mg_{0.3}Co_{0.45}Ni_{2.55-x}Fe_x ($x = 0, 0.1, 0.2, 0.3, 0.4$), based on which a series of alloys were represented with Fe content as Fe₀, Fe₁, Fe₂, Fe₃ and Fe₄, respectively. The experimental alloys were melted in a vacuum induction furnace. High purity helium with a pressure of 0.04 MPa was used as a protecting atmosphere to prevent the volatilization of magnesium during melting. The melt was poured into a copper mould, and a cast ingot was obtained. The part of the as-cast alloy was re-melted and quenched by melt-spinning with a rotating copper roller cooled by water. The quenching rate is defined as the linear velocity of the copper roller because it is too difficult to measure the real quenching rate, (i.e. the cooling rate of the sample when quenched). The quenching rates used in the experiment were 15, 20, 25 and 30 m·s⁻¹, respectively.

The cast ingot and quenched flakes were mechanically crushed and ground into powder with 47 μm in size for X-ray diffraction (XRD) analysis. The phase structures and compositions of the alloys were determined by XRD diffractometer (D/max/2400). The diffraction with the experimental parameters of 160 mA, 40 kV and 10°/min was performed with Cu Kα1 radiation filtered by graphite. The samples of the as-cast alloy were directly polished, and the flakes of the as-quenched alloy were enclosed in epoxy resin for polishing. The samples prepared were etched with a 60% HF solution. The morphologies of the as-cast and quenched alloys were examined by scanning electronic microscope (SEM). The powder samples of the as-quenched alloy were dispersed in anhydrous alcohol for observing the grain morphologies with transmission electronic microscope (TEM), and for determining the crystalline state of the samples with selected area electron diffraction (SAD). The granular morphologies of the alloy electrode before and after electrochemical cycle were inspected by SEM in order to reveal the mechanism of the efficiency loss of the alloy electrode.

Round electrode pellets of 15 mm in diameter were pre-

pared by cold-pressing a mixture of 0.2 g alloy powder and carbonyl nickel powder with a mass ratio of 1:4 and at a pressure of 354 MPa. After dried for 4 h, the electrode pellets were immersed in a 6 mol/L KOH solution for 24 h in order to wet fully the electrodes before the electrochemical measurement.

A tri-electrode open cell consisting of a metal hydride electrode, a NiOOH/Ni(OH)₂ counter electrode and a Hg/HgO reference electrode was used for testing the cycle stabilities of the experimental alloy electrodes. The electrolyte was a 6 mol/L KOH solution. The discharge voltage was defined as the voltage between the negative electrode and the reference electrode. In every cycle, the alloy electrode was charged with a constant current density of 600 mA·g⁻¹, and after resting for 15 min, it was discharged at the same current density to -0.500 V cut-off voltage. The environment temperature of the measurement was kept at 30 °C.

2 Results and Discussion

2.1 Structural characteristics

The XRD patterns of the as-cast and quenched (20 m·s⁻¹) alloys are shown in Fig.1, indicating that both alloys have multiphase structures consisting of two major phases, (La, Mg)Ni₃ and the LaNi₅, and a residual phase LaNi₂. The substitution of Fe for Ni results in an unconscious influence on the phase compositions of the alloys, and the major diffraction peaks of the LaNi₅ and the (La, Mg)Ni₃ phases in the alloys obviously tend to overlap with the increase of Fe content. Fig.1a displays a tendency that the substitution of Fe for Ni leads to an increase of the LaNi₂ phase in the as-cast alloy.

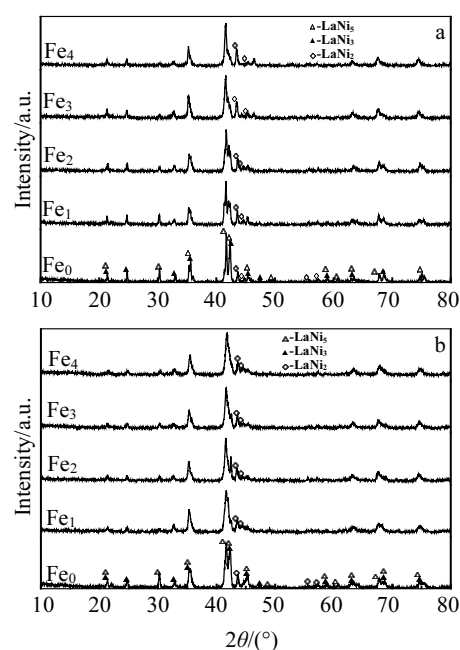


Fig.1 X-ray diffraction patterns of as-cast (a) and quenched (b) (20 m·s⁻¹) alloys

The lattice parameters of LaNi_5 and $(\text{La, Mg})\text{Ni}_3$ major phases in the as-cast and the quenched ($20 \text{ m}\cdot\text{s}^{-1}$) alloys are listed in Tab.1, which were calculated from the XRD data by the software Jade 6.0. The results indicate that the substitution of Fe for Ni in both alloys obviously enlarges the lattice parameters and the cell volumes of the major phases LaNi_5 and $(\text{La, Mg})\text{Ni}_3$, which is due to that the atom radius of Fe is larger than that of Ni compared with the as-cast. The rapid quenching makes the c -axis increased, but the a -axis and cell volumes of the main phases LaNi_5 and $(\text{La, Mg})\text{Ni}_3$ slightly decreased.

The SEM images of the as-cast and quenched alloys are shown in Fig.2. The result obtained by SEM with an energy dispersive spectrometry (EDS) indicates that all the experimental alloys are multiphase structure containing both $(\text{La, Mg})\text{Ni}_3$ and LaNi_5 phases, which is in agreement with that of XRD. Because the amount of the LaNi_2 phase is small and it attaches itself to the $(\text{La, Mg})\text{Ni}_3$ phase in the process of growing, it is difficult to observe the morphology of the LaNi_2 phase. As shown in Fig.2, the as-cast alloy consists of coarse grains and has poor composition homogeneity. The rapid quenching basically eliminates the above mentioned structural defects in the as-cast alloy. The grains of the as-quenched alloy exhibits a massive structure which is different from that of the as-quenched AB_5 -type electrode alloy that has a columnar structure^[9]. The substitution of Fe for Ni causes an obvious change in the morphologies of the as-cast alloys, and it leads to a significant refinement of the grains in the as-quenched alloy. A similar result was obtained in the investigation on the rare earth based AB_3 -type electrode alloy^[10].

The morphology and the crystalline state of the as-quenched alloy were examined by TEM, as shown in Fig.3. It is indicated in Fig.3 that the as-quenched ($20 \text{ m}\cdot\text{s}^{-1}$) Fe_0 alloy exhibits

a nanocrystalline and microcrystalline structure but Fe_2 and Fe_4 alloys trend to form a like amorphous structure, which can be detected by SAD. It seems to conflict with the result in Fig.1 due to that no amorphous phase was found by XRD. The reason would be that the like amorphous phase is formed at some selected locations in the as-quenched alloy and its amount is very small, so the XRD patterns do not clearly reveal its presence. Based on the result in Fig.3, it can

Table1 Lattice constants and cell volumes of LaNi_5 and $(\text{La, Mg})\text{Ni}_3$ major phases

Conditions	Alloys	Main phases	Lattice constants		Cell volume	
			a/nm	c/nm	V/nm^3	
As-cast	Fe_0	$(\text{La, Mg})\text{Ni}_3$	0.5053	2.4317	0.5377	
		LaNi_5	0.5031	0.4043	0.0886	
	Fe_1	$(\text{La, Mg})\text{Ni}_3$	0.5055	2.4362	0.5391	
		LaNi_5	0.5031	0.4045	0.0887	
	Fe_2	$(\text{La, Mg})\text{Ni}_3$	0.5061	2.4371	0.5406	
		LaNi_5	0.5036	0.4051	0.889	
	Fe_3	$(\text{La, Mg})\text{Ni}_3$	0.5069	2.4376	0.5424	
		LaNi_5	0.5040	0.4056	0.0892	
	Fe_4	$(\text{La, Mg})\text{Ni}_3$	0.5072	2.4381	0.5432	
		LaNi_5	0.5044	0.4060	0.0895	
	As-quenched ($20 \text{ m}\cdot\text{s}^{-1}$)	Fe_0	$(\text{La, Mg})\text{Ni}_3$	0.5046	2.4334	0.5366
			LaNi_5	0.5025	0.4052	0.0886
Fe_1		$(\text{La, Mg})\text{Ni}_3$	0.5051	2.4365	0.5383	
		LaNi_5	0.5028	0.4053	0.0887	
Fe_2		$(\text{La, Mg})\text{Ni}_3$	0.5057	2.4373	0.5397	
		LaNi_5	0.5031	0.4057	0.0889	
Fe_3		$(\text{La, Mg})\text{Ni}_3$	0.5062	2.4378	0.5401	
		LaNi_5	0.5036	0.4059	0.0891	
Fe_4		$(\text{La, Mg})\text{Ni}_3$	0.5067	2.4383	0.5421	
		LaNi_5	0.5041	0.4062	0.0894	

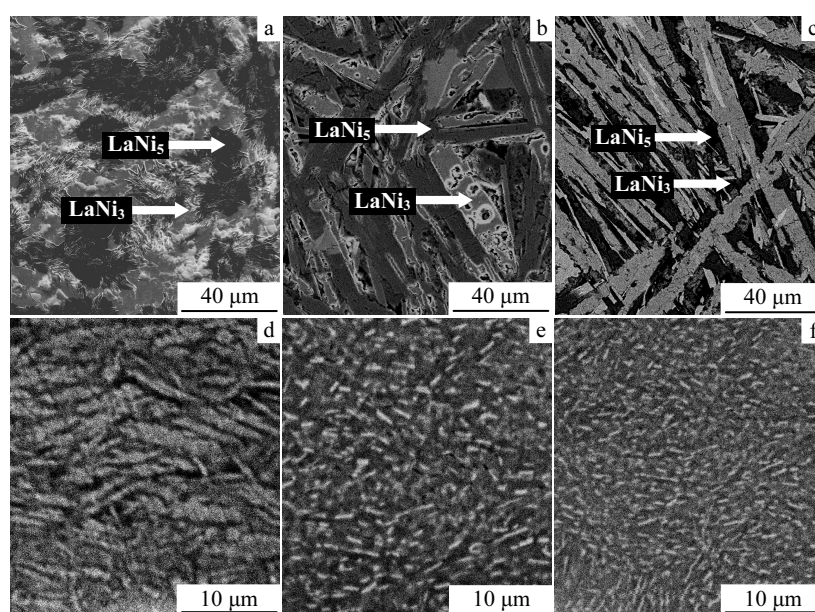


Fig.2 SEM images of the as-cast and quenched ($20 \text{ m}\cdot\text{s}^{-1}$) alloys taken : (a), (b), (c) as-cast Fe_0 , Fe_2 and Fe_4 alloys; (d), (e), (f) as-quenched Fe_0 , Fe_2 and Fe_4 alloys

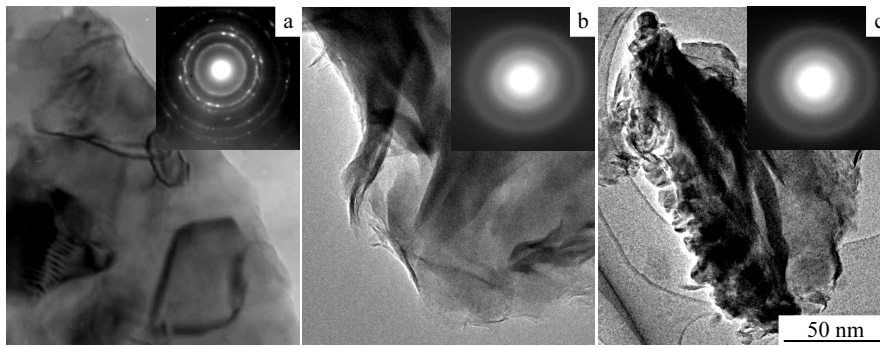


Fig.3 The morphologies and SAD patterns of the as-quenched alloys ($20 \text{ m}\cdot\text{s}^{-1}$) taken by TEM: (a) Fe_0 alloy, (b) Fe_2 alloy, and (c) Fe_4 alloy

be concluded that the substitution of Fe for Ni helps the formation of a like amorphous structure in the as-quenched alloy.

2.2 Cycle stability

The cycle life is defined as the cycle number after which the discharge capacity of an alloy at a current density of $600 \text{ mA}\cdot\text{g}^{-1}$ reduces to 60% of its maximum capacity. Fig.4 shows the influences of Fe substitution on the cycle stabilities of the as-cast and quenched alloys. It can be seen that the slopes of the curves of the as-cast and quenched ($20 \text{ m}\cdot\text{s}^{-1}$) alloys obviously drop with the increase of Fe content, implying that the substitution of Fe for Ni is helpful to improve the cycle stability of the alloys. Fig.5 shows the influences of the rapid quenching on the cycle stability of Fe_4 alloy. It can be seen that the slopes of the curves of Fe_4 alloy obviously fall with the increase of the quenching rate, meaning that the rapid quenching is favourable for improving the cycle stabilities of

the alloys. The cycle lives of the alloys as a function of Fe content are shown in Fig.6. The substitution of Fe for Ni clearly prolongs the cycle lives of the as-cast and quenched alloys. When Fe content rises from 0 to 0.4, the cycle life increases from 81 to 106 cycles for as-cast alloy, and from 99 to 152 cycles for the as-quenched ($20 \text{ m}\cdot\text{s}^{-1}$). Obviously, the substitution of Fe for Ni exhibits a much more significant influence on the cycle life of the as-quenched alloy than that of the as-cast one.

The cycle life of the alloys as functions of the quenching rate is shown in Fig.7, indicating that rapid quenching greatly

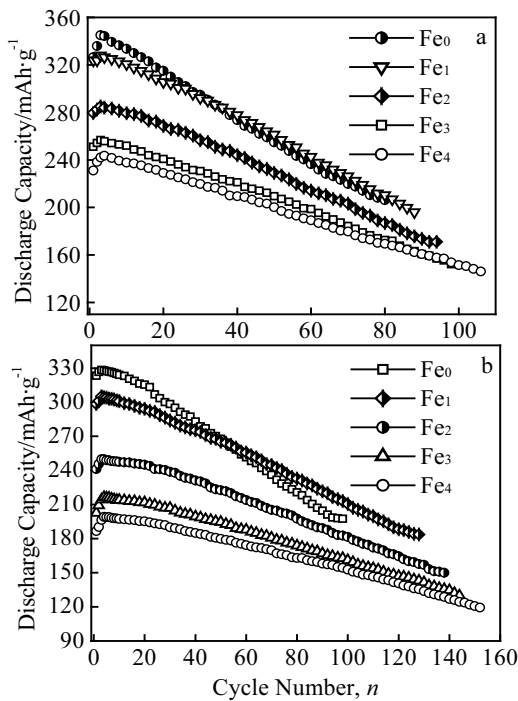


Fig.4 Evolution of the discharge capacity of alloys with cycle number: (a) as-cast and (b) as-quenched ($20 \text{ m}\cdot\text{s}^{-1}$) alloy

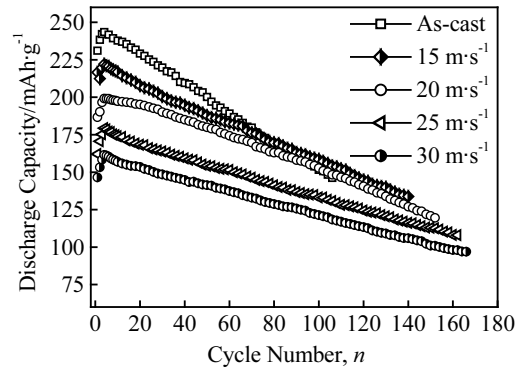


Fig.5 Evolution of the discharge capacity of Fe_4 alloy with cycle number

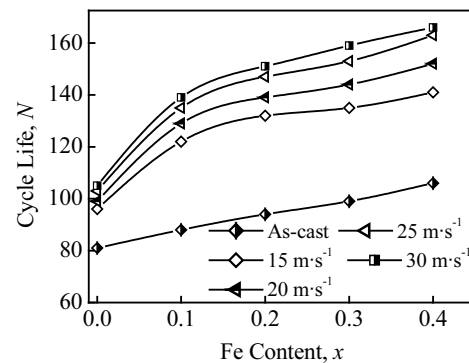


Fig.6 Evolution of the cycle life of the as-cast and quenched alloys with Fe content

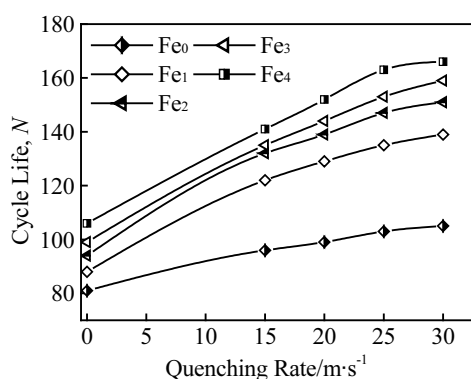


Fig.7 Evolution of the cycle life of the alloys with quenching rate

increases the cycle lives of the alloys. When the quenching rate increases from 0 (the as-cast is defined as the quenching rate of $0 \text{ m}\cdot\text{s}^{-1}$) to $30 \text{ m}\cdot\text{s}^{-1}$, the cycle life are prolonged from 81 to 105 cycles for Fe₀ alloy, and from 106 to 166 cycles for Fe₄ alloy. Apparently, the rapid quenching has a much large influence on the cycle life of the Fe-containing alloy than that of the Fe-free alloy.

The electrode failure is characterized by the decay of the discharge capacity and the drop of the discharge voltage. The literatures^[11,12] revealed that the fundamental reasons for the capacity decay of the electrode alloy are attributed to the pulverization and oxidation of the alloy during charging-discharging cycle. The internal stress in the lattice and the cell volume expansion, which are inevitable when hydrogen atoms enter into the interstitials of the lattice, are the real driving force that leads to the pulverization of the alloy. In order to correctly understand the mechanism of the efficacy loss of the experimental alloy electrode, the particle morphologies of the as-cast and quenched alloys before and after electrochemical cycle were observed by SEM as shown in Fig.8. It can be seen that the particle sizes and surface morphologies of the alloys have some changes after the electrochemical cycling, leading to the disappearance of the pointed shape of the particle and to the slight reduction of the particle sizes, and in addition, the cracks on the surface of the particle can clearly be seen in Fig.8c,

confirming that the pulverization of alloy particles takes place in the process of the charging-discharging cycle, but the pulverized extent of the alloy is much smaller than that of the AB₅-type alloy^[13]. It is noteworthy that a rough and porous layer can clearly be found on the surfaces of the particles after electrochemical cycling. It is most likely that it is the rough and flocculous layer that leads to the capacity deterioration of the alloy. The results analyzed by XRD as shown in Fig.9 reveal that the magnesium and lanthanum hydroxides were formed on the surfaces of the particles in strong alkaline solution. Thus, it can be concluded that the capacity deterioration of the alloy is mainly attributed to the oxidation of magnesium and lanthanum. Apparently, an effective approach to enhance the cycle stability of the La-Mg-Ni system electrode alloy is to improve the anti-corrosion and anti-oxidation capabilities of the alloys in an alkaline electrolyte.

Two explanations may be offered as the reason why the substitution of Fe for Ni enhances the cycle stabilities of the as-cast and quenched alloys. One is that the substitution of Fe for Ni enlarges the lattice parameters and the cell volumes of the alloys, decreasing the ratios of expansion/contraction of the alloys in the process of the hydrogen absorption/desorption, which means strengthening of the anti-pulverization capability of the alloys; the other is that the grain refinement of the electrode alloy caused by the substitution of Fe for Ni clearly intensifies the anti-pulverization capability, thereby improving the cyclic stability significantly. The grain refinement resulting from the rapid quenching is the major reason why rapid quenching enhances the cycle stability of Fe-free alloy. The grain refinement does not engender obvious influence on the anti-corrosion performance of the alloy. Therefore, the positive impact of the rapid quenching on the cycle stability of Fe-free alloy is very limited. For Fe-containing alloy, in addition to the refinement of the grains mentioned previously, the rapid quenching facilitates also the formation of a like amorphous structure, which significantly increases not only the anti-pulverization ability but also the anti-corrosion and anti-oxidation ones of the alloys^[14,15]. So, the cycle stabilities of the alloys are improved obviously.

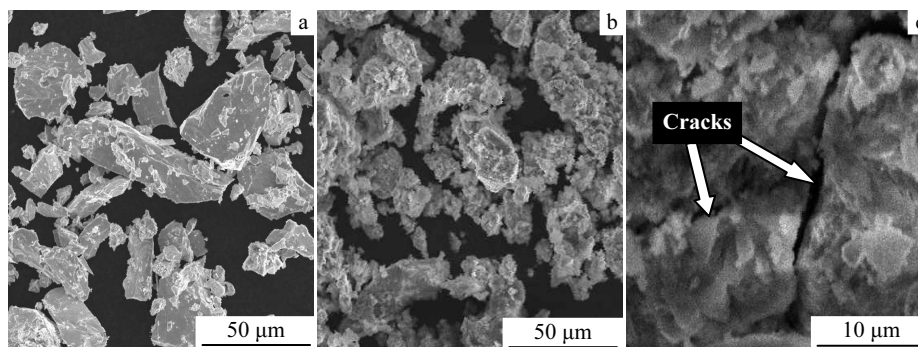


Fig.8 The granular morphologies of as-cast Fe₂ alloy before and after electrochemical cycle (SEM): (a) before cycle; (b) and (c) after cycle

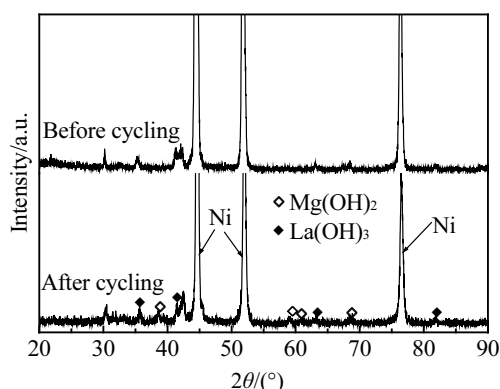


Fig.9 XRD patterns of the as-cast Fe₂ alloy before and after electrochemical cycle

3 Conclusions

1) The substitution of Fe for Ni engenders an unconscious influence on the phase compositions of the as-cast and quenched alloys, but leads to the significant refinement of the grains of the as-quenched alloy, is favourable to the formation of a like amorphous structure in the as-quenched alloy and leads to an obvious increase of the lattice constants and the cell volumes of the as-cast and quenched alloys.

2) The substitution of Fe for Ni obviously improves the cycle stabilities of the as-cast and quenched alloys, which is attributed to the increase of the cell volume and the refinement of the grains in the alloys produced by Fe substitution.

3) The positive impact of the substitution of Fe for Ni on the cycle life of the as-quenched alloy is much more significant than that of the as-cast one, which is due to the formation of a like

amorphous structure and the significant refinement of the grains in the as-quenched caused by the substitution of Fe for Ni.

References

- 1 Kadir K, Sakai T, Uehara I. *J Alloy Compd*[J], 1997, 257: 115
- 2 Kadir K, Kuriyama N, Sakai T et al. *J Alloy Compd*[J], 1999, 284: 145
- 3 Kadir K, Sakai T, Uehara I. *J Alloy Compd*[J], 1999, 287: 264
- 4 Kadir K, Sakai T, Uehara I. *J Alloy Compd*[J], 2000, 302: 112
- 5 Kohno T, Yoshida H, Kawashima F et al. *J Alloy Compd*[J], 2000, 311: L5
- 6 Pan H G, Liu Y F, Gao M X et al. *J Alloy Compd*[J], 2003, 351: 228
- 7 Liao B, Lei Y Q, Chen L X et al. *J Alloy Compd*[J], 2004, 376: 186
- 8 Pan H G, Yue Y J, Gao M X et al. *J Alloy Compd*[J], 2005, 397: 269
- 9 Zhang Y H, Dong X P, Wang G Q et al. *J Power Sources*[J], 2005, 140: 381
- 10 Zhao Y P, Zhang Y H, Wang G Q et al. *J Alloy Compd*[J], 2004, 388: 284
- 11 Liu Y F, Pan H G, Gao M X et al. *J Alloy Compd*[J], 2005, 403: 296
- 12 Chartouni D, Meli F, Züttel A et al. *J Alloy Compd*[J], 1996, 241: 160
- 13 Zhang Y H, Wang G Q, Dong X P et al. *J Power Sources*[J], 2005, 148: 105
- 14 Zhang Y H, Li B W, Ren H P et al. *J Alloy Compd*[J], 2007, 436: 209.
- 15 Ren H P, Zhang Y H, Li B W et al. *Mater Charact*[J], 2007, 58: 289

Fe 替代 Ni 对铸态及快淬态 La_{0.7}Mg_{0.3}Co_{0.45}Ni_{2.55-x}Fe_x (x = 0-0.4) 电极合金循环稳定性的影响

张羊换^{1,2}, 李保卫², 任慧平², 吴忠旺², 董小平^{1,3}, 王新林¹

(1. 钢铁研究总院, 北京 100081)

(2. 内蒙古科技大学, 内蒙古 包头 014010)

(3. 北京科技大学, 北京 100083)

摘要: 用铸造及快淬工艺制备了 La_{0.7}Mg_{0.3}Co_{0.45}Ni_{2.55-x}Fe_x (x = 0, 0.2, 0.3, 0.4) 电极合金, 研究了 Fe 替代 Ni 对合金循环稳定性及微观结构的影响。结果表明, Fe 替代 Ni 显著地改善合金的循环稳定性, 且 Fe 替代 Ni 对快淬态合金的循环稳定性具有更加显著的作用。试验合金具有多相结构, 包括 2 个主相 (La, Mg)Ni₃ 和 LaNi₅ 以及 1 个残余相 LaNi₂。Fe 替代 Ni 促进快淬态合金形成类非晶结构, 随 Fe 含量的增加, 快淬态合金的晶粒显著细化, 合金的晶格常数及晶胞体积显著增大。

关键词: La-Mg-Ni 系电极合金; Fe 替代 Ni; 快淬; 循环稳定性; 结构

作者简介: 张羊换, 男, 1959年生, 博士, 教授, 博士生导师, 钢铁研究总院功能材料研究所, 北京 100081, 电话: 010-62187570,

E-mail: zyh59@yahoo.com.cn